CORROSION BEHAVIOR OF STAINLESS STEEL IN SOLID OXIDE FUEL CELL SIMULATED GASEOUS ENVIRONMENTS

M. Ziomek-Moroz
U.S. Department of Energy, Albany Research Center, 1450 Queen Avenue, SW, Albany, OR 97321 E-mail: moroz@alrc.doe.gov; Telephone: (541) 967-5943; Fax: (541) 967-5914

B. S. Covino, Jr., G. R. Holcomb, S. D. Cramer, S. A. Matthes, S.J. Bullard, J. S. Dunning, D. E. Alman, R. Wilson
U.S. Department of Energy, Albany Research Center, 1450 Queen Avenue, SW, Albany, OR 97321

Prabhakar Singh
Pacific Northwest National Laboratory, 902 Battelle Boulevard, P.O. Box 999, Richland, WA 99352
E-mail: prabhakar.singh@pnl.gov; Telephone: (509) 375-5945; Fax: (509) 375-2167

Abstract

Significant progress in reducing the operating temperature of solid oxide fuel cells (SOFC) from ~1000°C to ~ 750°C may permit the replacement of currently used ceramic interconnects by metallic interconnects in planar SOFCs (PSOFC). The use of metallic interconnects will result in a substantial cost reduction of PSOFCs. The interconnects operate in severe gaseous environments, in which one side of the interconnect can be exposed to hydrogen and the other side to air or oxygen at temperatures up to 800°C. Similar environmental conditions can exist in devices used for separating hydrogen from CO after reforming methane and steam. Type 304 stainless steel was selected for this base line study aimed at understanding corrosion processes in dual gas environments. This paper discusses the oxidation resistance of 304 stainless steel exposed to a dual environment gas at 800°C. The dual environment consisted of air on one side of the specimen and 1% hydrogen in nitrogen on the other side. The surface characterization techniques used in this study were optical and scanning electron microscopy, as well as various x-ray techniques.

Introduction

Fuel cells are energy conversion devices that generate electricity and heat by converting chemical energy into electrical energy without any combustion process.[1] The electrochemical reactions occur between a fuel gas, such as pure hydrogen, and atmospheric oxygen. In an SOFC, oxygen ions diffuse from the air cathode side through a conductive electrolyte to the anode side, where they react with the hydrogen of the fuel gas and form water. During this half – cell reaction, electrons are released, and flow through an outer electrical circuit. A single cell typically produces up 0.5 to 0.9 V. In order to obtain higher voltages, these cells are stacked together and electrically connected in series via interconnects, also called bipolar separators. Figure 1 shows a schematic of a planar SOFC stack.[2]

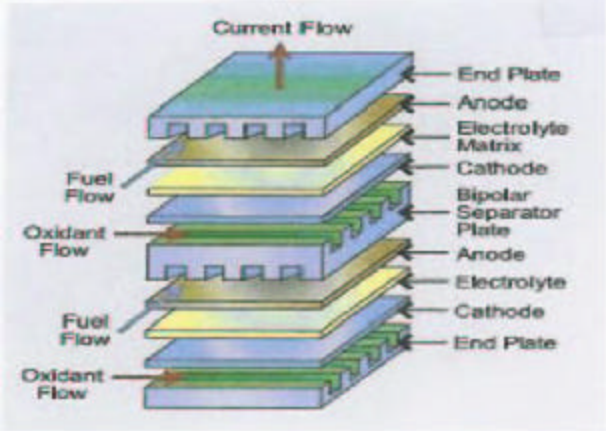

Figure 1. Schematic of planar solid oxide fuel cell stack

The interconnect is a critical component. In addition to providing electrical connection between individual cells, it serves as a gas separation barrier to prevent mixing of the fuel (e.g. H_2) and atmospheric air.[1] Significant progress in the reducing operating temperature of SOFC from ~1000°C to ~ 750°C may allow for less expensive metallic materials. A metallic interconnect must meet the following requirements:[3]

- It must possess sufficient chemical and physical stability to withstand a dual environment (atmospheric air on the cathode side and fuel on the anode side)
- It must have good electrical and thermal conductivity
- It must be able to withstand repeated thermal cycling from room temperature to 800°C.
- It must be flexible enough to withstand thermal expansion mismatch or if brittle the thermal expansion coefficient must well matched to the cell components, i.e., cathode, anode, and electrolyte.

Also, metallic materials used for separating hydrogen from CO after reforming methane and steam reactors must exhibit excellent corrosion resistance in dual environments with temperatures up to 800°C and pressures ranging from 50-150 psi. Figure 2 shows an example of the SOFC components of a combined-cycle power plant, indicating the main processes occurring in the system.[4] Type 304 stainless steel[5], due to its excellent corrosion resistance, was selected for the base line study aimed at understanding corrosion processes in dual gas environments.

This paper discusses the corrosion behavior of commercial 304 stainless steel exposed to air on one side of the specimen, and 1% hydrogen in nitrogen on the other side. Tubular specimens at temperatures varying from ambient to 800°C and pressures from atmospheric to 150 psi were used. Surface characterization techniques, including optical and scanning electron microscopy, as well as various x-ray techniques were used in this study.

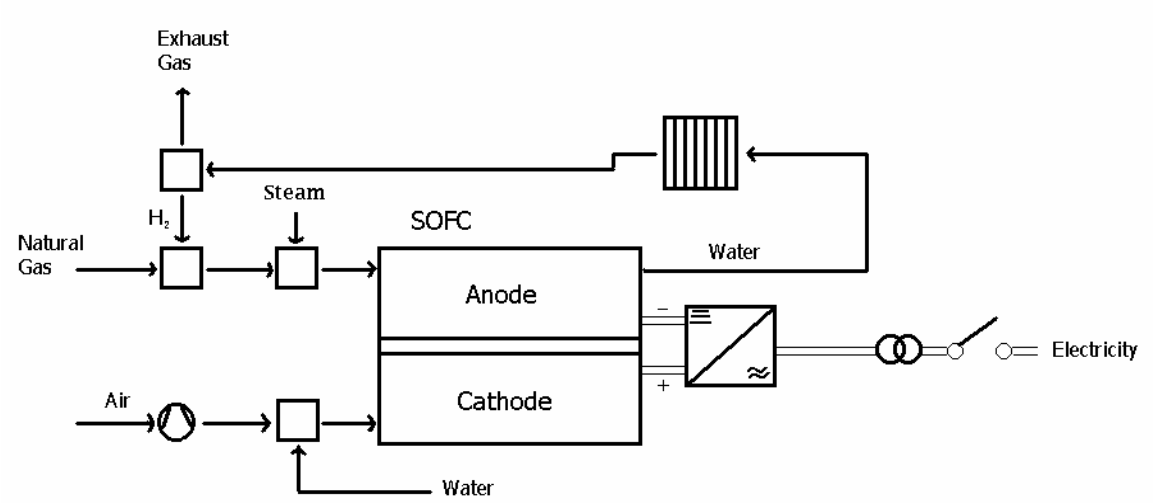

Figure 2. Schematic of SOFC components of a combined-cycle power plant

Experimental Procedures

Experiments were performed on commercial 304 stainless steel tubular specimens shown schematically in Figure 3.

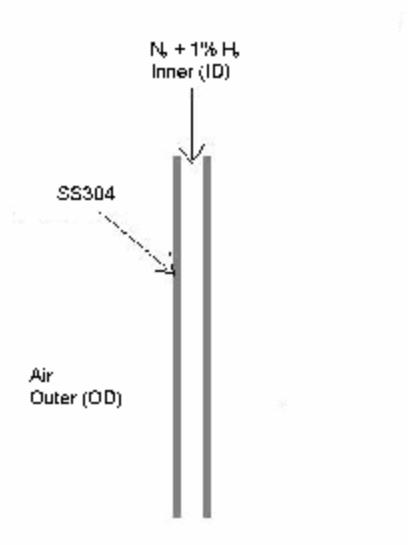

Figure 3. Schematic of 304 SS tubular specimen

The experiments were performed on the materials as received. In the experiment, the inner specimen surface (ID) was exposed to 99% N_2 + 1% H_2 for a period of one year; simultaneously, the outer surface (OD) was exposed to air for the same period. During this time, the specimen was held at the following temperature values: 600, 700 and 800^{o}C. At each temperature, the system was pressurized to 50, 100, and 150 psi. Also, the material was exposed to cyclic heating ranging from ambient to 800^{o}C.

After the experiment, the specimen surfaces were observed using optical and scanning (SEM) microscopy. The SEM, equipped with an energy dispersive X-ray

(EDX) analyzer, was used determine the morphology and chemical distribution of different elements in the corrosion products (scales). In order to determine the stoichiometry of the compounds present in the scales, X-ray photoelectron spectroscopy (XPS) was used. The crystalline phases present in the scales were determined using X-ray diffraction (XRD).

Results and Discussion

Outer Surface

The SEM micrograph of the longitudinal outer surface of the specimen exposed to the air is shown in Figure 4.

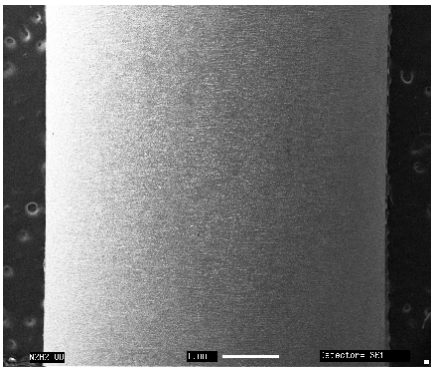

Figure 4. SEM micrograph of longitudinal outer surface of specimen (16X)

As can be seen, the scale formed uniformly on the surface. Figure 5 shows the SEM micrograph of the same surface at a higher magnification. The topography of the surface is relatatively rough, compared to the initial surface.

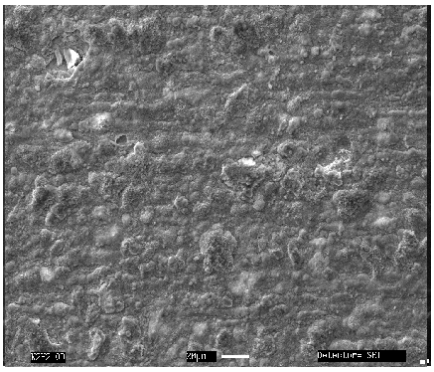

Figure 5. SEM micrograph of longitudinal outer surface of specimen (400X)

This roughness is caused by the presence of oxidation products unevenly distributed on the surface , as shown in Figure 6. There are no cracks visible under the scale.

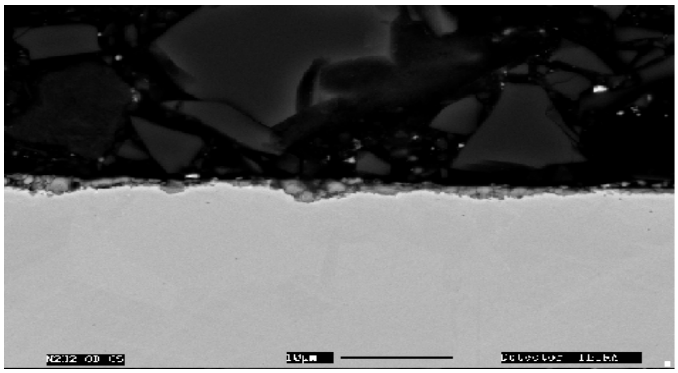

Figure 6. SEM micrograph showing outer surface cross-section of specimen (400X)

The EDX analysis (Figure 7) detected the presence of Fe and small amount of Cr. Also, the XPS survey spectrum (Figure 8) shows that the spectrum is dominated by the strong Fe 2p3 and O 1s peaks. The Cr 2p3 peak is very small. This indicates that the scale mainly contains iron oxides.

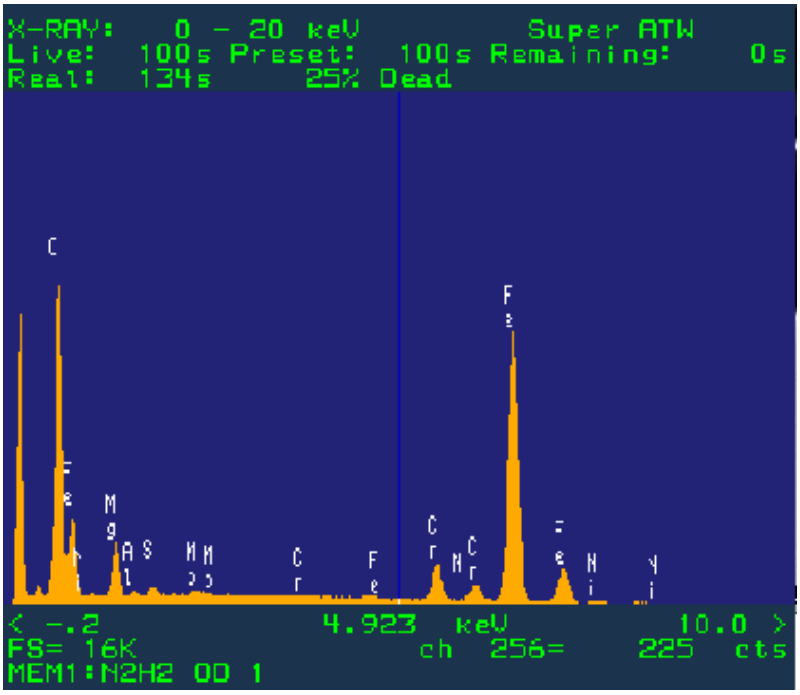

Figure 7. EDX spectrum of longitudinal outer surface

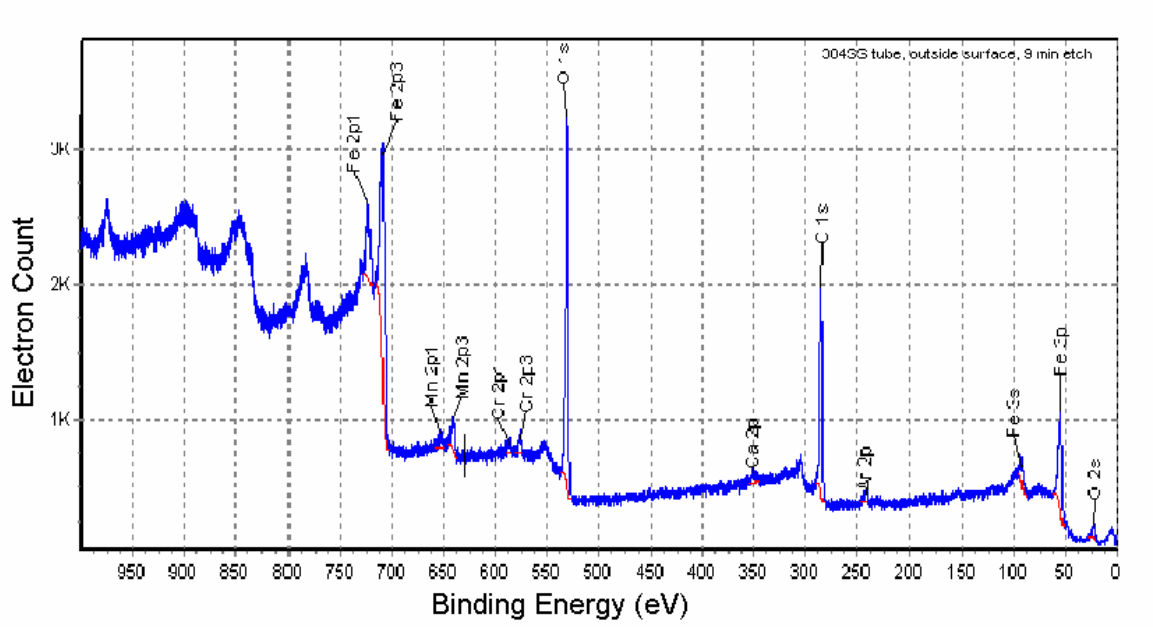

Figure 8. XPS survey spectra for longitudinal outer surface

The XRD analysis of the scale revealed the main crystalline compound is hematite (Fe_2O_3). Also, some traces of magnetite (Fe_3O_4) and chromia (Cr_2O_3) were present.

Inner Surface

The SEM micrograph of the longitudinal inner surface of the specimen exposed to 99 %N_2 and H_2 is shown in Figure 9.

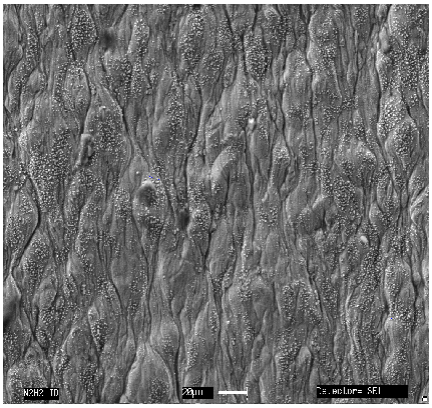

Figure 9. SEM micrograph of longitudinal inner surface (400X)

The topography of the inner surface is quite different from that of the outer surface. The surface is ridged, which appears to be associated with the manufacturing processes of the tubular specimens.

As with the outer surface cracks are also not observed in the SEM micrograph of the cross-section shown in Figure 10.

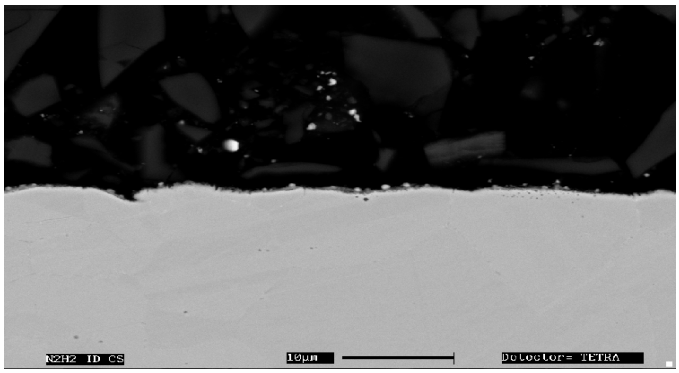

Figure 10. SEM micrograph showing inner surface cross section (400X)

The EDX analysis of the corrosion products detected a lower amount of Fe and a higher amount of Cr in comparison to the scale formed on the outer surface. Comparison of the XPS survey spectra for the inner and outer surfaces shown in Figure 11 also indicates a higher concentration of Cr and a lower concentration of Fe in the scale formed on the inner surface.

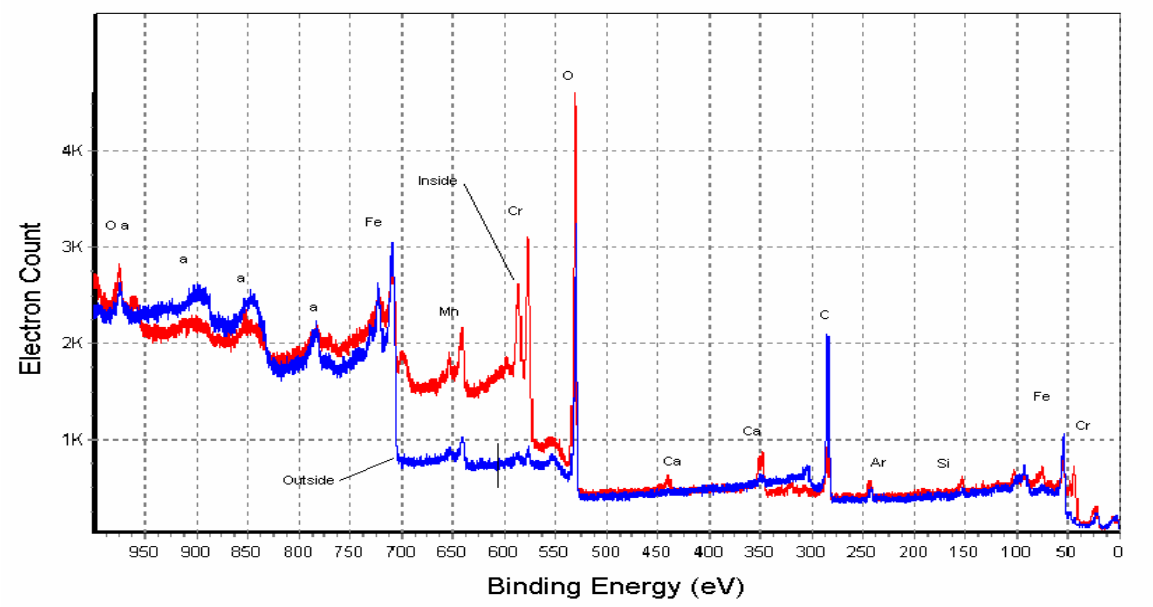

Figure 11. Comparison of XPS survey spectra for outer (air) and inner (H_2+ N_2) surfaces

The XRD analysis of the scale revealed the main crystalline compounds are magnetite (Fe_3O_4) and chromia (Cr_2O_3). Although the inner surface was exposed to the reducing environment during the experiment, the presence of the oxide scale was detected. This is caused by exposure of the material to air during the experimental setup.

The difference between the chemical composition of the scales formed on the outer and inner surfaces is associated with different mechanisms of corrosion during simultaneous exposure to oxidizing and reducing environment. Sing and Yang[6] suggest the following reactions in fuel (e.g. hydrogen) and oxidant:

$$MO + 2(H) = M + H_2O$$
$$M + 0.5O_2 = MO$$

Different stability of Fe_3O_4 in comparison to Cr_2O_3 may explain the presence of mainly Fe_3O_4 and Cr_2O_3 in the scale formed on the inner surface. Low concentration of Cr_2O_3 in the outer surface may be caused by chromia evaporation[6]:

$$Cr_2O_3 + 0.5O_2 + 2H_2O \rightarrow 2CrO_2(OH)_{2(g)}$$

Conclusions

- SEM analysis of the surface indicates uniform formation of scale in air and N_2 + 1% H_2.
- XRD results show the presence of the following crystalline oxides on inner (N_2 + H_2) and outer (air) surfaces: magnetite Fe_3O_4 and chromia Cr_2O_3 on the inner surface; hematite Fe_2O_3 was found on the outer surface.
- Fe_3O_4 and Cr_2O_3 are the predominate oxides formed on the inner surface; Fe_2O_3 with traces of Cr_2O_3 and Fe_3O_4 were the oxide formed on the outer surface.
- XPS results show the presence of Cr on the inner surface, and its significant reduction on the outer surface. This may indicate Cr evaporation from the outer surface.
- The oxide scale present on the inner surface was formed due to exposure of the material to air during the experimental setup.

Acknowledgements

The authors acknowledge the assistance of Dale Govier and Keith Collins of the U.S Department of Energy, Albany Research Center, and John Murphy of Drexel University

References

1. Fuel Cell Handbook, fifth edition, U.S. Department of Energy, Office of Fossil Energy, National Energy Technology Laboratory.
2. SECA Program Plan – Making Fuel Cells Available to America, U.S. Department of Energy, National Energy Technology Laboratory, Pacific Northwest National Laboratory.
3. Diane England, Private Communication.
4. Heinz Termuelhen, 100 Years of Power Plant Development, ASME Press, New York, 2001.
5. Z.G. Yang, K.S. Weil, D.M. Paxton, and J.W. Stevenson, 2002 Fuel Cell Seminar Abstracts, p.522.
6. Prabhakar Singh & Z. Gary Yang, Thermo chemical analysis of Oxidation and Corrosion Processes in High Temperature Fuel Cells, Presented at 131st TMS Annual Meeting. Seattle, WA. February 18, 2002.